

Article

A Dual Active-Passive Coating with Intumescent and Fire-Retardant Properties Based on High Molecular Weight Tannins

Francisco Solis-Pomar¹, Andrés Díaz-Gómez² , María Elizabeth Berrío² , Jesús Ramírez²,
Andrés Felipe Jaramillo³ , Katherina Fernández⁴, David Rojas², Manuel Francisco Melendrez^{2,5}
and Eduardo Pérez-Tijerina^{1,*}

¹ Facultad de Ciencias Físico-Matemáticas, Universidad Autónoma de Nuevo León, San Nicolas de los Garza, Nuevo León 66451, Mexico; francisco.solisp@uanl.edu.mx

² Interdisciplinary Group of Applied Nanotechnology (GINA), Hybrid Materials Laboratory (HML), Department of Materials Engineering (DIMAT), Faculty of Engineering, University of Concepcion, 270 Edmundo Larenas, Box 160-C, Concepción 4070409, Chile; andresdiaz.qind@gmail.com (A.D.-G.); maelibeni2018@gmail.com (M.E.B.); alframirez09@gmail.com (J.R.); davrojas@udec.cl (D.R.); mmelendrez@udec.cl (M.F.M.)

³ Department of Mechanical Engineering, Universidad de La Frontera, 01145 Francisco Salazar, Temuco 4780000, Chile; andresfelipe.jaramillo@ufrontera.cl

⁴ Laboratory of Biomaterials, Department of Chemical Engineering, Faculty of Engineering, University of Concepcion, Barrio Universitario s/n, P.O. Box 160-C, Concepción 4030000, Chile; kfernandez@udec.cl

⁵ Unidad de Desarrollo Tecnológico, 2634 Av. Cordillera, Parque Industrial Coronel, Box 4051, Concepción 4191996, Chile

* Correspondence: eduardo.perez@uanl.edu.mx



Citation: Solis-Pomar, F.; Díaz-Gómez, A.; Berrío, M.E.; Ramírez, J.; Jaramillo, A.F.; Fernández, K.; Rojas, D.; Melendrez, M.F.; Pérez-Tijerina, E. A Dual Active-Passive Coating with Intumescent and Fire-Retardant Properties Based on High Molecular Weight Tannins. *Coatings* **2021**, *11*, 460. <https://doi.org/10.3390/coatings11040460>

Academic Editor: Ivan Jerman

Received: 6 March 2021

Accepted: 29 March 2021

Published: 16 April 2021

Publisher's Note: MDPI stays neutral with regard to jurisdictional claims in published maps and institutional affiliations.



Copyright: © 2021 by the authors. Licensee MDPI, Basel, Switzerland. This article is an open access article distributed under the terms and conditions of the Creative Commons Attribution (CC BY) license (<https://creativecommons.org/licenses/by/4.0/>).

Abstract: In this study, the tannins extracted from the *Pinus radiata* bark were used to develop an active-passive dual paint scheme with intumescent (IN) and fire-resistant (FR) behaviors. The properties of the coating were observed to depend on the concentration of high-molecular-weight tannins (H-MWT) incorporated into the formulation. At high concentrations (13% *w/w*), the coating exhibits fire-retardant properties due to the generation of a carbonaceous layer; however, at low concentrations (2.5% *w/w*), it generates an intumescent effect due to the formation of a carbonaceous foam layer. The dual IN-FR scheme was evaluated against fire by flame advance tests, carbonization index, mass loss, and intumescent effect, and was also compared to a commercial coating. The dual scheme presented good mechanical properties with a pull-off adhesion value of 0.76 MPa and an abrasion index of 54.7% at 1000 cycles, when using a coating with a high solid content (>60%) and the same thickness as those of the commercial coatings. The results of the fire resistance test indicate that the dual scheme generates a protective effect for wood and metal, with an excellent performance that is comparable to that of a commercial intumescent coating.

Keywords: fire-resistant coating; tannin; eco-friendly; intumescent flame retardant; *Pinus radiata*

1. Introduction

Construction safety considering accidents due to fire is an ever-present concern, requiring the development of new materials capable of offering better fire protection and therefore providing longer escape and rescue times [1,2]. For this purpose, intumescent and fire-retardant coatings have received great attention. They offer thermal protection to metallic building structures such as steel, which can lose their mechanical and structural properties when subjected to high temperatures during a fire, leading to the collapse of the building [2]. In the same way, wood is another structural material that is also susceptible to fire, as it is highly combustible and requires fire protection systems [3–5].

For a long time, great effort has been invested in the search for materials that provide properties against fire, to develop protection systems such as fire-retardant and intumescent

coatings. The difference between these two systems is that in a fire-retardant coating, the combustion process on the coated surface culminates in the generation of non-bulky carbonaceous material, whereas in intumescent coatings, a carbonaceous foam is mainly generated that protects the surface from the action of fire [3,6]. The formation of the protective layer and, therefore, the increase in the time that the structure resists flame depends on the coating composition. Generally, these coatings are composed of three main components: a carbon source (commonly polyalcohols), an acid source responsible for the dehydration of the carbon source and also for triggering the intumescence reaction (acting as a catalyst), and a blowing or foaming agent, which is responsible for producing gases that lead to the expansion of the coating. The intumescence reaction is consolidated from a series of chemical reactions that are carried out by the effects of the increase in temperature. It begins with the thermal decomposition of the acid source, which subsequently interacts with the hydroxylated compound (polyalcohol) [7,8], and then, finally, the blowing agent decomposes and releases the gases responsible for the swelling of the coating [9]. In contrast, the fire-retardant reaction involves only the first two steps, since no blowing agents are required [10].

Nowadays, the development of new coatings must be ecologically conscious as well as safe for human health. Considering these requirements, the use of biomass can be a good potential source of carbon for the coatings. Tannins, for example, have aromatic and hydroxyl rings in their structure, which are very important for good intumescence and thermal stability, and they can be excellent raw materials that provide a good alternative to petroleum-based chemicals [11–13]. Tannin extracts are mixtures of polyphenols, simple phenols such as gallic acid, esters of a sugar (mainly glucose), gallic and digallic acids, as well as flavonoids such as catechin and taxifolin, among others. The presence of gallic acid as a basic structure in hydrolyzable tannins makes it an ideal raw material for the preparation of coatings [14,15]. In the field of bioproducts, the application of these extracts to prepare coatings, composites, and prepolymer components in polymeric systems has become a hot topic in research [16].

Several researchers have extensively studied the physicochemical mechanisms, flammability, and characterization of intumescent coatings. However, no research has been reported on the development of coating schemes using fire-retardant and intumescent layers formulated from tannins. In this context, studies have been reported in which coatings were developed from ammonium phosphates with lignin and expandable graphite as pigments to improve the fire protection performance of intumescent coatings, with the thermal protection evaluated on steel substrates. Lignin may be a good option to replace nonrenewable sources in intumescent coatings, since in this study, substrates with 10% *w/w* of this material reached 230 °C after 30 min of exposure to the flame [4]. Chen et al. [17] manufactured a fire-resistant coating from the thermal degradation of phosphate acrylate monomers and the formation of phosphoric acid, which increased the development of carbon on the surface of the coated substrate. Likewise, Wang et al. [18] used ammonium phosphate to generate intumescent coatings resistant to acid attack and aging by acid erosion. However, petroleum-derived compounds continued to be used in these studies.

In this study, extracts of high-molecular-weight tannins were obtained from the bark of *Pinus radiata*. After extraction, the bark does not lose its heat capacity and can be used in industrial boilers. Therefore, this process is sustainable. The extracts were characterized and used to prepare two types of formulations separately: one with fire-retardant (FR) properties and the other with intumescent (IN) properties. The coating scheme was used on both wood and steel substrates, where the intumescent was the inner layer and the fire-retardant was the outer layer.

2. Materials and Methods

The reagents used for the formulation of the coatings were as follows: pentaerythritol (PER, Sigma-Aldrich, San Luis, MO, USA), 2,4,6-triamino-1,3,5-triazine (MEL: Melamine, Merck, SA, Darmstadt, Germany), dimethyl sulfoxide (DMSO, Sigma-Aldrich, San Luis,

MO, USA), high- and low-molecular-weight tannins (H-MWT and L-MWT), ammonium phosphate dihydrate (MAP, Merck, SA, Darmstadt, Germany), sodium polyphosphate (SPP, Merck, SA, Darmstadt, Germany), and styrene acrylic dispersion (Acronal S716, BASF, Ludwigshafen, Germany), whereas the commercial coatings for comparison were Retardant 77 (C-FR, commercial fire retardant paint, Chilcorrofin[®], Santiago, Chile) and Firewall 200 (C-IN, commercial intumescent paint, Tricolor[®], Santiago Chile).

2.1. Extraction and Characterization of the H-MWT

The tannins were obtained by liquid–liquid extraction using polar solvents. To do so, the dried and ground *Pinus radiata* bark was placed in contact with a 3:1 (*v/v*) ethanol/water mixture for 2 h at 120 °C. Subsequently, the volatile solvent was removed by room temperature evaporation under 5.0 kPa using a vacuum system. Finally, the H-MWT and L-MWT were separated by sedimentation and dried by lyophilization [19]. Characterization of the extracts was performed by reversed-phase high performance liquid chromatography (RP-HPLC) with a diode array detector (DAD) and a mass spectrometer (MS) using a 1% acetic acid mobile phase (*v/v*) (phase A) and acetonitrile (phase B) at a flow rate of 0.8 mL/min. A calibration curve was constructed using catechin solutions (0.10–1.00 g/L) and taxifolin (0.06–1.00 g/L) as standards [14].

2.2. Optimization of Base Formulation and Effect of the Addition of H-MWT as a Carbon Source

The FR and IN coating formulas were prepared using a base formulation (BF) (Table 1). The formulas were initially optimized by varying the percentages of the active components (Table S1), where MAP was used as the acid catalyst, ME as the foaming agent, and PER as the polyol or carbon source. The optimized coating was chosen by evaluating its ability to generate intumescent or fire-retardant effects against a thermal stimulus. The foaming level and the carbonization index were determined following the procedure described in the ASTM D3806 standard on a wooden substrate. H-MWT was added to the optimized coating to evaluate its effect as a complementary polyol in the formulation (Table 2). Other components were held fixed, and the amount of tannins added varied between 2.5% and 26%. All formulations were made as follows: All solids were ground in a mortar prior to dispersion, added to the dispersion reactor together with the solvent and the dispersant additive, then mechanically mixed at 1000 rpm for 4 h using a cowles stirrer and ceramic grinding beads until a particle size of 4 Hegman was obtained, according to the ASTM D333 standard. Subsequently, complementary components were added, and the mixture was stirred at 1400 rpm for 2 h. Finally, the acrylic binder was added, and the mixture was stirred at 800 rpm for 10 min. The coating formulations were stored until they were applied on wood and steel substrates.

Table 1. Basic formulation (BF).

Component	(%)
Solvent	43.5
Polyol	8.3
Catalytic acid	23.1
Foaming agent	7.4
Complementary components	8.3
Polymeric matrix	9.3

Table 2. Variation of the percentage content of PER, H-MWT, ME, and MAP in compositions.

Component	Variation Ratio (%)				
	FT1	FT2	FT3	FT4	FT5
Ratio MAP/PER	1.5	1.5	1.5	1.5	1.9
MAP	25.0	25.0	25.0	25.0	25.0
PER	15.0	15.0	15.0	15.0	15.0
ME	14.0	14.0	14.0	14.0	8.0
H-MWT	13.0	26.0	5.8	2.5	2.5

The fire-resistance, intumescence test, and carbonization index were carried out on wooden substrates. For this, medium-density fiberboard (MDF)(Arauco cellulose company, Santiago, Chile) plates with dimensions of $150 \times 150 \times 9 \text{ mm}^3$ and steel substrates of $150 \times 100 \times 3 \text{ mm}^3$ were used, and were painted with the coatings using a brush and dried at $25 \text{ }^\circ\text{C}$ for 24 h. For the flame resistance test, the painted wood was placed on a metal support with an inclination of 28° with respect to the horizontal and 3 cm from a flame supplied by a torch. The substrate temperature was measured using a thermocouple on the unpainted area, that is, contrary to the area where the flame was applied. Once the successful formulations were determined with the addition of H-MWT, these were evaluated by varying their thickness (100 μm , 200 μm , and 300 μm).

2.3. Dual Coating Scheme with FR and IN Properties

Based on the results obtained in the previous stages, where tannins were added as a carbon source (Table 2), two coatings were selected, one with IN and another with FR properties. The dual effects of these coatings were evaluated in an IN–FR coating scheme and were compared to commercial fire-resistant and intumescent coatings. The application of the coating scheme was carried out using a conventional spray gun on wood and steel substrates, with a thickness of 300 μm of dry film for each formulation. Each coating application was allowed to dry for 12 h at $25 \text{ }^\circ\text{C}$. The surface preparation of the metallic substrates was carried out according to the standards established by the Steel Structures Painting Council (Pittsburgh, PA, USA), applying sections SP1 and SP5.

2.4. Determination of the Mechanical, FR, and IN Properties of the Active–Passive Dual Coating

The effectiveness against flame of the coating scheme was quantified by evaluating the resistance to temperature, permanence, and advance of the flame, following the ASTM D3806 standard on wood and metal substrates. Additionally, the carbonization index and mass loss were evaluated by the ASTM D1360 standard for wood substrates. The mechanical properties were evaluated by determining the abrasion resistance using a Taber Abraser (BYK-Instrument, Pompano Beach, FL, USA) model 5135 with a load of 1 kg, abrasion stones of low-medium hardness type CS-10, and rotation at 60 rpm, according to the ASTM D4060 standard. Adherence was also evaluated by tensile testing using the PosiTes AT-A (DeFelsko Corporation, Ogdensburg, NY, USA) according to the ASTM D4541 standard, and flexibility was determined according to the ISO 1519 standard by bending $160 \text{ mm} \times 60 \text{ mm}$ plates at 180° with a BYK 5710 cylindrical mandrel (BYK-Instrument, Pompano Beach, FL, USA) with diameters of 2.0 mm, 8.0 mm, and 20.0 mm. The cupping test was performed according to ISO 1520 using a BYK PF-5405 machine (BYK-Instrument, Pompano Beach, FL, USA). To guarantee adequate adhesion to the metal substrates, they were initially painted with an acrylic primer with a thickness of $32.7 \pm 5.3 \text{ } \mu\text{m}$, then the formulated coatings were applied to the primer. Additionally, a commercial fire-retardant coating (Retardant 77 coded as C-FR) (Chilcorrofin[®], Santiago, Chile) and a commercial intumescent (Firewall 200 coded as C-IN) (Tricolor[®], Santiago Chile). were used as controls.

3. Results and Discussion

3.1. Chemical Characterization of H-MWT

The tannins extracted from *Pinus radiata* showed a yield of 6.2% for H-MWT and 15.4% for L-MWT per 100 g of bark. According to the RP-HPLC-MS analyses, the H-MWTs presented molecular weights of approximately 5000 Da, with 41.9 ± 2.9 mg catechin and 21.5 ± 2.0 mg taxifolin per gram of extract. These results are consistent with those of Ma et al. [20], who characterized the condensed tannins present in the Cabernet Sauvignon seed extract by UHPLC-Q-ToF-MS (ultra-high performance liquid chromatography-quadrupole time-of-flight mass spectrometry), finding molecular weight values of approximately 6000 Da. Another study developed by Yang et al. [21] determined that the molecular weight distribution of tannins and the availability of hydroxyl groups defines their reactivity. They evaluated the reactivity of formaldehyde against tannin extracts of 1500 to 4800 Da, obtained from aromatic shrubs of the *Myricaceae* family known as bayberry. Their results showed that tannins with the highest average molecular weights (between 3900 and 4100 Da) had the best reactivity. Regarding the content of total phenols, Montoya et al. [13] reported that the total phenol content (g gallic acid/g extract) was 0.603 ± 0.002 in L-MWT and 0.528 ± 0.003 in H-MWT. In this work, the H-MWT tannin extracts used in the formulation of FR and IN coatings acted as carbonaceous layer-forming agents and not as alcohol-supplying agents in the reaction with the catalyst.

3.2. Optimization of Base Formulation and Effect of H-MWT as a Complement to the Carbon Source

To optimize the percentages of the main components in the formulation, it is necessary to understand the intumescence process, which depends on the thermal decomposition temperature of the components involved. Thus, the reaction process begins with the decomposition of the catalytic acid that subsequently reacts with the polyol, dehydrating it and forming a phosphate ester and H₂O. Subsequently, the decomposition of MEL occurs, which generates the evolution of NH₃ and CO₂ gases and the consequent foaming of the previously formed complex [9]. In the case of using sodium polyphosphate (SPP) as a catalyst agent, it presents a decomposition temperature of approximately 593 °C [22]. This is a higher value when compared to the MEL present in the pigment mixture of the tested base formulation (300 °C) [23], which leads to the generation of CO₂ and ammonium vapors from the decomposition of MEL. The above occurs prior to the decomposition of the acid and to the reaction with the polyol, for which no carbonaceous layer or intumescence is generated.

When using MAP, decomposition occurs at temperatures below the decomposition temperature of SPP (210 °C) [24,25], generating the phosphoric acid necessary for reaction with the carbon source (PER), which decomposes into short chains at 250 °C [26,27]. In this way, the type of polyphosphate used in the formulation indisputably marks the intumescent reaction, because of its ability to generate the main compound that acts as a catalyst for the dehydration reaction of the polyol and formation of the ester. Wang et al. studied the thermal decomposition of coatings developed with ammonium polyphosphate, which decomposes at temperatures of 290 °C [28]. This allows it to react with PER at these temperature ranges, generating water and ammonium gas [18]. Therefore, from the results obtained, it is observed that using SPP in the base formulation as an acid source (BF-SPP) does not generate a voluminous carbonaceous layer, unlike when using MAP (BF-MAP) (BF: base formulation), which generates superior intumescence properties in the coating when exposed to fire (see Figure S1). For this reason, MAP was chosen as the acid catalyst in this work.

Table S1 presents the formulation results from varying the main component (MAP, PER, and MEL) percentages. Three molar ratios were used of phosphate:polyol (MAP:PER), 1:1, 2:1, and 4:1, to alter the reactivity of the polyol. In the first case, there is a reaction between a MAP molecule with only one OH group from PER. In the second case, there is a reaction with two MAP molecules, and in the last one, all OH from the PER are involved,

forming a polymer complex [29]. In the latter case, the 4:1 ratio contemplates the reaction between each OH group of the PER molecule with a MAP molecule. This relationship is unlikely due to the possible steric hindrance, leading to excess phosphate. Therefore, a greater probability of a complete reaction is expected when using molar ratios where there are excess phosphate groups in the medium. Thus, the MAP/PER percentage ratios with indices of 2.7, 1.9, and 1.5 presented better properties of fire resistance and intumescence. When altering the ratio of foaming agent (MEL) used, greater gas evolution was observed when the percentage was increased. The expansion area of the flame on the sample surface was smallest for BF2, and the most voluminous carbonaceous layer was seen with BF3 (see Figure S2). Therefore, a greater amount of foaming agent and carbon source presented a better response to the flame, forming a carbon layer of greater thickness and less area affected by the flame. However, in BF4, the amount of acid present in the formulation was controlled by a MAP/PER ratio < 1.0 , which led to a loss of carbonaceous foaming capacity due to excess polyol and a deficiency of phosphate groups in the medium that form the phosphate ester complex with OH groups (Figure S2). In this way, MAP/PER ratios > 1 , as presented in formulations BF1, BF2, and BF3, allow for a complete reaction and better intumescence properties.

Other factors had to be considered prior to creating the formulation with H-MWT, as previous wetting of the tannins was required to improve the rheological properties of the formulations due to their hydrophilicity. The water absorption results of the H-MWT and L-MWT extracts (Figure S3) indicated that, by increasing the contact time of the particles with the aqueous medium, their swelling increased until reaching an absorption maximum of 9 and 31 times their weight in a period of 77 and 207 h for H-MWT and L-MWT, respectively. After this saturation time, the amount of water absorbed plateaued due to the complete swelling of the tannin particles. Since adsorption is a physical phenomenon influenced by the surface area of the particles, it was expected that the L-MWT would adsorb greater amounts water because they have shorter molecular chains compared to the H-MWT. Regarding these results, in the formulations with H-MWT, 9 L of water were required for each kg of tannins to moisten all the particles in the established period of time, while adjusting the viscosity of the formulation with rheological agents until obtaining values of 127 KU (10–15% dilution at 15 °C). After formulation, the coating was applied on opacity drawdown charts to observe the covering power and wet film thicknesses of 400 μm , as shown in Figure 1. Those layers with fire-retardant properties presented greater opacity and covering power, with brown tones due to the high amount of tannins in the formulation, whereas the surfaces coated with the intumescent formulation presented lighter shades.

The intumescent and fire-retardant properties of the coatings developed with H-MWT were determined by the response of both wood and steel to flame. It was found that the FT1 and FT5 (FT: tannin formulation) coatings formulated according to Table 2 showed intermediate properties between the fire retardant and intumescent coatings (Figure 1). For the FT1 formulation, exposure to fire triggered the formation of a carbonaceous layer on the surface that acted as an active thermal barrier. For FT2, a spongy carbonaceous layer with an intumescent response was formed on the coated surface. The quantification of this response was carried out by measuring the mass loss of the wood substrates and comparing to the uncoated wood substrate mass loss of $14.7 \pm 0.1\%$. The mass loss measurements showed better results for the FT1 and FT5 coating formulations in Table 3, with values of $7.3 \pm 0.5\%$ and $9.3 \pm 0.8\%$, respectively. It should be noted that FT1 did not show carbonaceous foam formation, but there was less mass loss. This is due to the fact that it contained a large amount of tannins, exceeding the optimal value of the phosphate/polyol ratio, providing a carbon source that acts as a thermal insulator and preventing the advance of the flame. Furthermore, when high amounts of H-MWT are added to the formulation, the phosphate/polyol ratio is not the only factor to take into account for the generation of intumescence, since it is necessary to use a greater amount of MEL. This is because the tannin molecule has available OH groups that react with the phosphoric acid produced

by the decomposition of MAP, forming esters in the same way as PER. Additionally, these molecules in the formulation form complex structures after the reaction is activated by temperature, which turns into carbonaceous foam with a minimal amount of added MEL. According to studies by Braghiroli et al. [30], three-dimensional structures can be formed after the reaction between tannins and ammonia derivatives, so the H-MWT used here also forms complex structures not only due to the presence of phosphates from the catalyst, but also due to the presence of ammonium ions.

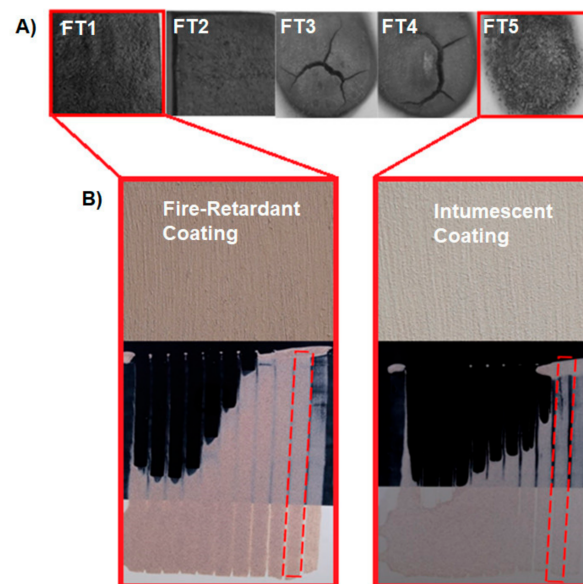


Figure 1. (A) Flame response of coatings with different PER/MAP/ME ratios. (B) Film properties; hiding power, wet thickness, and drainage for coatings.

Table 3. Mass loss percentage for coating formulations.

Mass Loss (%)					
Wood	FT1	FT2	FT3	FT4	FT5
14.7 ± 0.1	7.3 ± 0.5	10.2 ± 0.2	11.7 ± 0.9	11.5 ± 0.7	9.3 ± 0.8

On the other hand, the FT5 formulation also presented a low percentage of mass loss and generated foaming, an effect attributable to the lower amount of tannins, not unbalancing the MAP/PER ratio and favoring the growth of the carbonaceous layer. The results show that the best formulations were FT1 and FT5, which presented MAP/H-MWT ratios of 1.6 and 8, respectively. The coating obtained with FT1 had a high tannin content and exhibited fire-retardant behavior, whereas FT5 had intumescent properties due to its lower tannin amount, allowing the generation of a carbonaceous foam with greater volume when exposed to fire.

3.3. Evaluation of the Mechanical and Functional Properties of Active–Passive Coatings (IN-RF)

3.3.1. Evaluation of Flame Resistance of Coatings on Wood Substrates

The previous testing results allowed for the establishment of a range of optimal values to generate intumescent and fire-retardant effects from the FT5 and FT1 formulations, respectively. Therefore, the FT5 formulation that had the best intumescent properties was coded as IN and the best fire retardant as FR. When evaluating the coatings independently on wood (Figure 2), it was found that by increasing the coating thickness, higher fire resistance times were achieved, as seen for the following values of 10.0 ± 0.1 s (101.6 μm), 9.9 ± 0.1 s (210.5 μm), and 29.9 ± 0.1 s (303.8 μm) for the FR coatings and 10.0 ± 0.1 s (100.5 μm), $20. \pm 0.1$ s (220.6 μm), and 30.0 ± 0.1 s (301.6 μm) for the IN coatings. Likewise,

the temperature reached on the back face of the wooden substrate after exposure to flame was reduced by both coatings; 16.2 ± 0.7 , 16.3 ± 0.4 , and 14.7 ± 0.3 °C for FR, and 39.1 ± 0.1 , 14.8 ± 0.8 , and 13.9 ± 0.8 °C for IN, respectively (see Table 4). These results are noteworthy, as a layer of 100 µm for both coatings does not protect the wood; however, with thicknesses of 300 µm, the FR and IN coatings presented significant fire resistance. Comparing the resistance time of the two evaluated coatings with the commercial ones, the formulated coatings were found to have intermediate values between those presented by the commercial intumescent (C-IN) (Chilcorrofin[®], Santiago, Chile) with 70.0 ± 0.1 s and the commercial fire-retardant (C-FR) (Tricolor, Santiago Chile) with 29.8 ± 0.1 s, using thicknesses of approximately 300 µm. Comparing these results, the C-FR coating presented weak properties of resistance to temperature, therefore at least twice the thickness needed to be applied for results similar to those obtained with the FR coating developed.

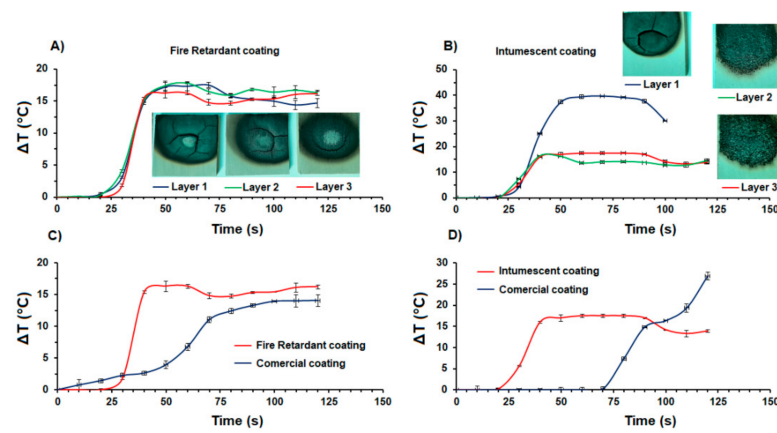


Figure 2. Resistance to temperature increase on wood substrates depending on the thickness of the coatings: (A) fire-retardant coating (FR), (B) intumescent coating (IN), (C) commercial fire-retardant coating (C-FR), and (D) commercial intumescent coating (C-IN).

Table 4. Functional properties of fire retardant and intumescent coatings on wood and steel substrates.

Coating	Wood					Steel	
	Thickness (µm)	Fire Resistance Time (s)	Substrate Back Side Temperature (°C)	Mass Loss (g)	Carbonization Index (%)	Thickness (µm)	Substrate Back Side Temperature (°C)
FR1	101.6 ± 14.6	10.0 ± 0.1	16.2 ± 0.7	7.4 ± 0.6	37.1 ± 2.1	104.6 ± 15.3	189.1 ± 10.5
FR2	210.5 ± 5.8	10.0 ± 0.1	16.3 ± 0.4	6.5 ± 0.5	33.1 ± 2.2	210.4 ± 11.9	187.0 ± 13.3
FR3	303.8 ± 16.1	30.0 ± 0.1	14.7 ± 0.3	5.2 ± 0.6	23.7 ± 2.9	307.1 ± 12.7	165.9 ± 11.1
IN1	100.5 ± 13.5	10.0 ± 0.1	39.1 ± 0.1	9.35 ± 0.5	41.9 ± 2.7	106.6 ± 19.0	387.9 ± 10.5
IN2	220.6 ± 15.9	20.0 ± 0.1	14.8 ± 0.8	7.8 ± 0.6	22.7 ± 2.6	235.1 ± 10.4	225.1 ± 15.2
IN3	301.6 ± 22.7	30.0 ± 0.1	13.9 ± 0.8	6.5 ± 0.7	19.6 ± 3.0	305.6 ± 11.5	181.2 ± 13.2
C-IN	317.1 ± 11.5	70.0 ± 0.1	26.9 ± 0.3	0.2 ± 0.1	4.6 ± 0.7	310.1 ± 7.2	298.8 ± 55.6
C-FR	305.3 ± 7.6	29.8 ± 0.1	14.1 ± 0.2	7.4 ± 1.0	19.9 ± 1.9	300.4 ± 30.5	301.5 ± 68.9
IN–FR Scheme	612.1 ± 9.7	66.4 ± 0.1	12.6 ± 1.2	3.5 ± 0.3	20.0 ± 5.7	639.4 ± 54.6	147.4 ± 15.31
Wood	-	10.0 ± 0.1	20.0 ± 1.9	13.5 ± 1.2	52.5 ± 5.4	-	-
C-IN	650.3 ± 23.5	79.9 ± 0.0	5.8 ± 3.1	0.4 ± 0.3	9.2 ± 1.4	630.9 ± 55.6	238.9 ± 20.1

In contrast, for the dual IN–FR coating on the wood substrates, intermediate properties were observed between the C-IN and C-FR coatings (see Figure 3 and Table 4). In this coating scheme, a passive layer was found to reduce the increase in temperature, and a spongy carbonaceous layer was formed inside. Thus, the temperature resistance time was increased for IN–FR to 66.4 ± 0.1 s (612.1 ± 9.7 µm) in relation to the individual IN3 and FR3 coatings. The value obtained by the IN–FR scheme was close to that of the C-IN coating at similar thickness, which presented a time of 79.9 ± 0.0 s for 650.3 ± 23.5 µm.

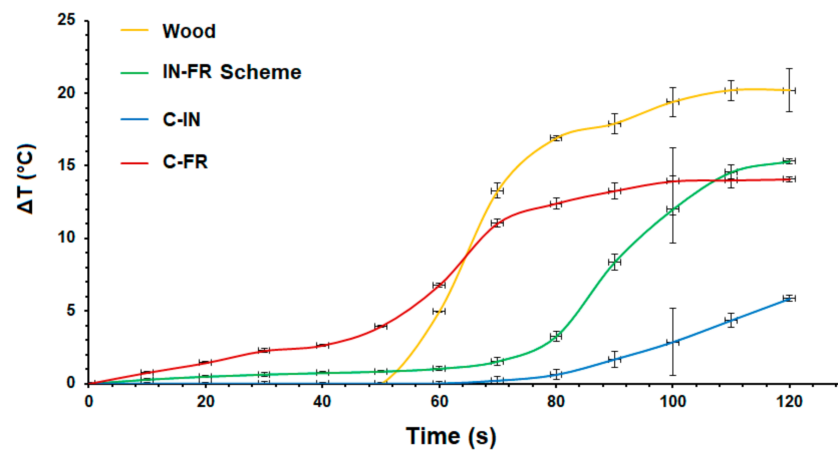


Figure 3. Resistance to temperature increase of the dual scheme (IN–FR) on wood substrates compared to commercial coatings.

In order to obtain the carbonization index of the wood substrates coated with the FR and IN formulations (Figure 4a), they were exposed to a direct flame and subsequently cut vertically and horizontally to quantify the advance of the flame in the transverse direction of the substrate (Figure 4b). For the dual active–passive IN–FR scheme, a flame advance into the substrate of 3.4 ± 1.1 mm and a surface foam generation of 9.9 ± 0.2 mm thick were observed. When comparing these results to the commercial coatings, the C-IN coating presented the best results because the flame only advanced 1.6 ± 0.2 mm into the substrate and generated a carbonaceous layer of 17.5 ± 1.2 mm. The FR coating did not generate surface foam, but it did prevent the advance of the flame in the transverse area of the substrate. Although the dual system (IN–FR) did not present the best results compared to the commercial coatings, it did generate a blocking effect to the flame advance compared to the uncoated wood substrate, which presented a flame advance of 6.8 ± 3.3 mm. Another effect of the dual scheme was that by eliminating the source of fire, there was a self-extinguishing of the flame on the substrate.

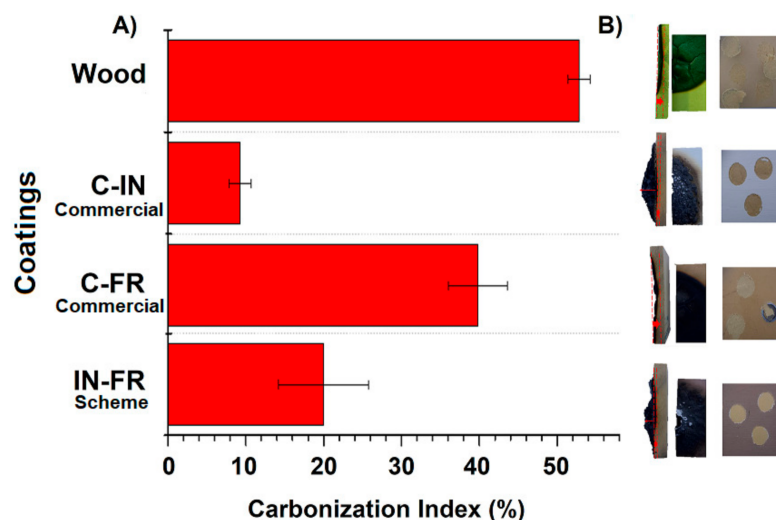


Figure 4. (A) Carbonization index of the dual scheme (IN–FR) on wood substrates with respect to the respective commercial coatings (C-IG and C-IN). (B) Resistance to detachment by adherence of the dual scheme (IN–FR) on wood substrates.

When evaluating the mass loss of the wood substrates coated with the FR (FT1) and IN (FT5) separately, these decreased with increasing thickness of the protective coating, resulting in values of $5.2 \pm 0.6\%$ and $6.5 \pm 0.7\%$ with dry thicknesses of 303.8 ± 16.1 μm

and $301.6 \pm 22.7 \mu\text{m}$, respectively (see Figure S4 and Table 4). These results were superior to the commercial coatings (C-FR and C-IN) and uncoated substrate, which presented values of $7.4 \pm 1.0\%$, $0.2 \pm 0.1\%$, and $19.9 \pm 1.9\%$, respectively. When comparing the values of the carbonization indices, the formulated coatings presented the best values, only surpassed by C-IN. The carbonization indices were as follows: $23.7 \pm 2.9\%$, $19.6 \pm 3.0\%$, $19.9 \pm 1.9\%$, $4.6 \pm 0.7\%$, and $52.5 \pm 5.4\%$ for FR, IN, C-FR, C-IN, and uncoated wood, respectively.

The results obtained for the individual coatings were similar to those obtained for the dual system, in which a mass loss of $3.5 \pm 0.3\%$ and carbonization index of $20.0 \pm 5.7\%$ were obtained. However, there was a slight improvement when combining both effects (fire-retardant and intumescent) in a single painting scheme (see Figure 4). Silveira et al. [16] reported similar values using a fire-resistant epoxy coating based on *Acacia mearnsii* tannins on steel sheets with 1.5 mm of dry film thickness, reaching stabilization at $\sim 150^\circ\text{C}$, which presents promising properties in terms of fire protection. Yang et al. [31] evaluated the fire resistance capacity of tannins obtained from *Dioscorea cirrhosa* applied on silk textiles, showing a decrease in the flammability of the fabrics at low extract concentrations (37.5 g/L). Figure 5 shows a field test where the IN-FR scheme on a wood substrate was evaluated. Commercial coating (C-IN) and uncoated wood were used as control. This preliminary test indicated that the tannin-based coating scheme with fire resistance properties can be used as potential additives in these formulations.



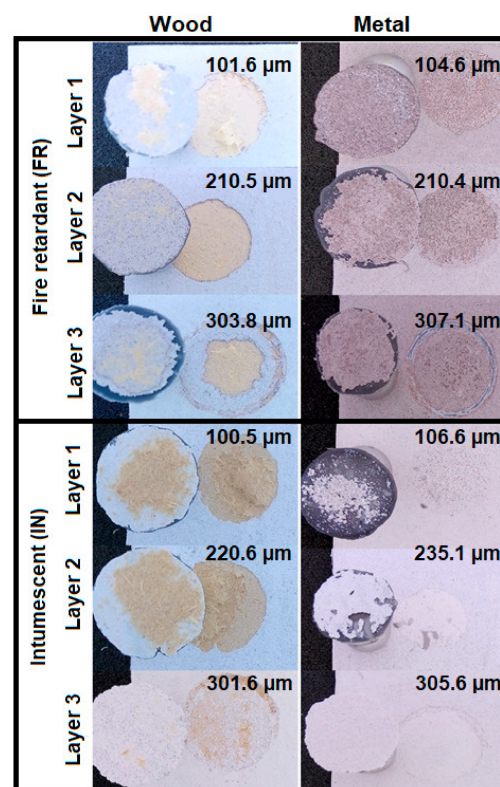
Figure 5. Field test of the dual scheme (IN-FR) on wood.

3.3.2. Evaluation of the Mechanical Properties of Coatings on Wood Substrates

The pull-off adhesion mechanical properties of the formulated coatings on wood substrates were evaluated, and the results are presented in Figure 6 and Table 5. From the results obtained for the individual coatings (FR and IN), it was observed that as the thickness increased, the adherence to the substrate decreased, presenting failures mainly of the adhesive type in the wood-coating interface, with tensile force values of $\sim 1.4 \text{ MPa}$.

Table 5. Tensile strength according to adhesion tests of fire retardant and intumescent coatings on wood and steel substrates.

Coating/No. Layers	Tensile Strength (MPa)			
	Wood	Type of Failure	Metal	Type of Failure
FR1	1.48 ± 0.02	100% adhesive	1.30 ± 0.06	100% cohesive
FR2	1.25 ± 0.43	100% adhesive	1.13 ± 0.16	100% cohesive
FR3	0.79 ± 0.17	60% adhesive	0.74 ± 0.02	100% cohesive
IN1	1.42 ± 0.05	100% adhesive	1.70 ± 0.09	20% cohesive
IN2	1.31 ± 0.06	100% adhesive	1.03 ± 0.06	80% cohesive
IN3	0.79 ± 0.01	100% cohesive	0.87 ± 0.03	100% cohesive

**Figure 6.** Resistance to detachment by adherence for fire retardant and intumescent coatings on wood and metal depending on the thickness.

For the dual scheme, the pull-off adhesion properties were compromised due to an increase in the thickness of the coating, further decreasing its adherence to the wood substrate. The resulting values were 0.76 ± 0.01 MPa of tensile force with 100% cohesive failure. Figure 4b shows the results of the adhesion and foaming tests on wooden substrates for the evaluated coatings. These results are consistent with those found by Tudor et al. [32].

3.3.3. Evaluation of Fire Resistance of Coatings on Metal Substrates

When evaluating the flame behavior of coatings formulated and applied on a metallic substrate, an improvement in the fire-retardant and intumescent properties was observed when increasing the thickness of the applied coatings. After exposure to flame, a whitish non-spongy layer was generated by FR and a dense spongy layer was formed by IN. The results of foaming and profiles of the temperature increase versus the exposure to flame are presented in Figure 7. At the end of the fire exposure, the temperatures reached on the back of the metallic substrates with fireproof coatings were 189.1 ± 10.5 , 187.0 ± 13.3 , and

165.9 ± 11.1 °C for the three thicknesses evaluated (100, 200 and 300 μm , respectively) (see Table 4). With the commercial coatings, temperatures up to 373.2 ± 12.2 °C were reached. The formation of carbonaceous foam from the IN coating on the metal substrates produced a decrease in the temperature on the back face, from 387.9 ± 10.5 °C with 100 μm to 181.2 ± 13.2 °C for 300 μm . Puri et al. [33] obtained temperatures of 220 °C from a coating of high thickness (1000 μm) on steel through the formulation of an intumescent vinyl coating with the addition of hollow ceramic spheres. This temperature is higher than those obtained by coatings formulated with thinner tannins. Therefore, fire retardant and intumescent coatings with the addition of H-MWT show promise for superior protection of both wood and metal surfaces. Similarly, the fire resistance of the dual scheme (IN-FR) showed a maximum temperature of 147.4 ± 15.31 °C on the back face of the metal substrate. These values were much lower than those obtained by the IN and FR formulations separately. This is owing to the fire resistance dual effect from the formation of a carbonaceous layer and the generation of a superficial foam, preventing the transfer of heat to the metallic substrate (see Figure 8).

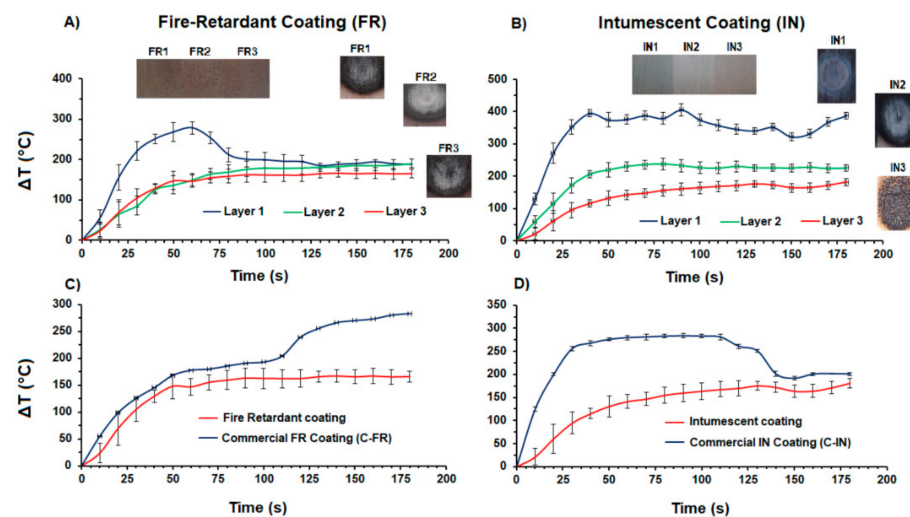


Figure 7. Resistance to temperature increase on steel substrates depending on the thickness of the coatings: (A) fire-retardant coating (FR), (B) intumescent coating (IN), (C) commercial fire-retardant coating (C-FR), and (D) commercial intumescent coating (C-IN).

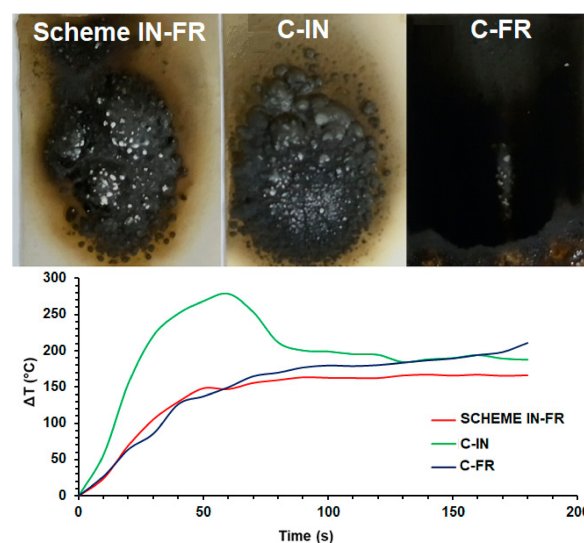


Figure 8. Resistance to temperature increase of the dual scheme (IN-FR) on steel substrates compared to commercial coatings.

3.3.4. Evaluation of the Mechanical Properties of Coatings on Metal Substrates

The results of adhesion testing of the coated metal substrates are shown in Table 6. Similar to the behavior of the wood substrates, the values decreased with the increasing thickness of the coatings. However, in all cases there was cohesive failure between the layers (see Figure S5), with values around 1.3 and 1.7 MPa for the first FR and IN layers with thicknesses of 110.6 ± 9.5 and 105.1 ± 10.3 μm , respectively. The above indicates that there was strong adhesion of the coatings to the metallic substrates. Baldissera et al. [4] evaluated the adhesion strength of polyaniline-based intumescent coatings with the addition of lignin in the formulation. Their results showed forces of 1.48 MPa for coating thicknesses around 1700 μm . This indicates that, following their formulation, thicknesses are required that are at least 15 times greater to obtain similar results reported in the present work. Likewise, Kwang et al. [34] used intumescent coatings with thicknesses of approximately 2000 μm on metal and evaluated the adhesion force by tensile testing on a universal machine. Their results showed values of approximately 1.45 MPa. Because both authors deposited the coatings on bare metal, a strong influence of the preparation of the metallic surface was evidenced by the anchoring of fire retardant and intumescent coatings. For the adhesion tests of the dual scheme (IN-FR), the main failure was cohesive between the internal layers of the coating, with tensile forces of 0.7 ± 0.1 MPa (Table 6).

Table 6. Adhesion tests on steel substrate.

Coating	Tensile Strength (MPa)	Type of Failure
IN-FR	0.70 ± 0.14	25% cohesive IG/15% adhesive IG glue/60% cohesive IN
C-IG	3.02 ± 0.32	30% adhesive IG primer/70% adhesive IG glue
C-IN	0.98 ± 0.04	100% cohesive

These results are similar to those of the IN and FR coatings tests. However, commercial fire-retardant coatings, as they consist of acrylic varnishes, bind strongly to the surface of the previously applied primer, showing high adhesion values (3.0 ± 0.3 MPa). These results show that tannin-based paints have good adhesion properties on metal substrates; however, they are identified as having better adhesion (mainly chemical-type adhesion) on wood substrates because of the strong interaction between the polyphenols of the tannins and the lignocellulosic functional groups of the wood surface. On the other hand, the evaluation of cracking and flexibility in the cupping tests presented greater resistance to detachment and cracking by increasing the thickness on the metal plate, with values of 0.35 mm (101 μm thickness), 0.80 mm (210 μm thickness), and 0.95 mm (303 μm thickness) for the FR and 0.75 mm (100 μm thickness), 0.83 mm (220 μm thickness), and 0.98 mm (301 μm thickness) for the IN coatings (see Figure 9). However, the flexural elasticity of the coatings was compromised with greater thicknesses, as their detachment was evident with a curvature diameter of 2 mm. The coatings of the IN-FR scheme showed a gradual advance in cracking, with visible deformations at mandrel diameters even less aggressive than 8 mm. The elastic response showed cracking of the coating film in the curvature generated in the metal substrates, as observed in Figure 10. This behavior was attributed to the presence of a high content of solids, as these generated a decrease in mechanical properties compared to the commercial coating (C-FR), which had a PVC content of ~35% and excellent elastic properties, maintaining its integrity at lower diameters (2 mm). However, overall, the flexibility results obtained compared to the commercial coatings are acceptable.

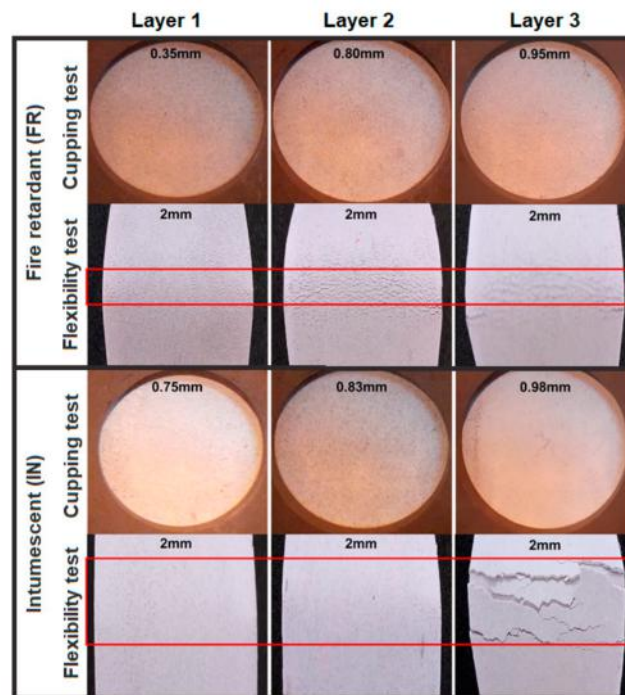


Figure 9. Resistance to cupping and bending tests for fire-retardant (FR) and intumescent (IN) coatings on steel substrates with different thicknesses.

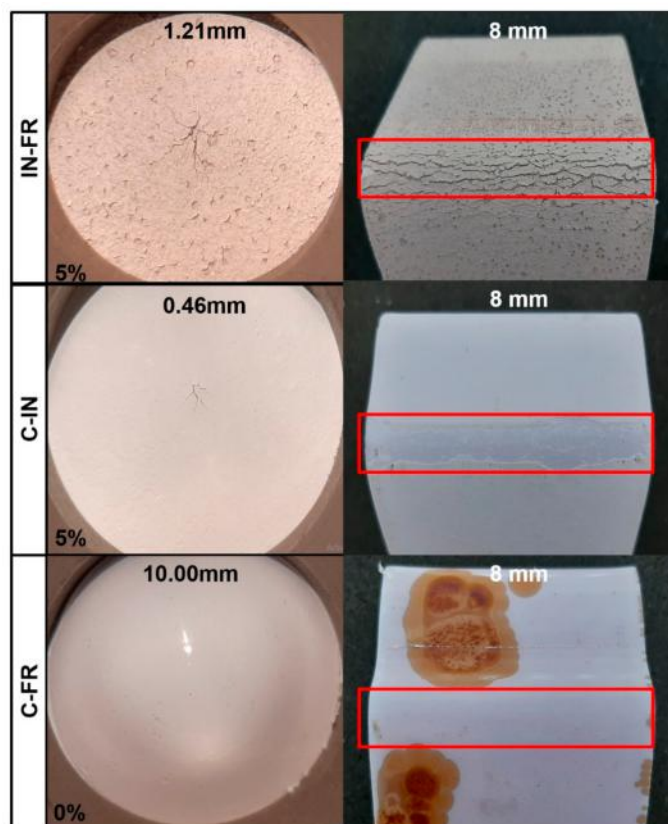


Figure 10. Resistance to cupping and bending tests for the dual scheme (IN-FR) on steel substrates compared to commercial coatings.

Regarding other mechanical results, the wear index of the steel decreased as the number of coating layers increased for both FR and IN (Figure S6). For thicknesses

of 300.2 ± 25.5 (for FR) and 315.2 ± 36.0 μm (for IN), similar properties of resistance to abrasion wear were found, with values only 14% lower for IN with respect to FR: 118.2 ± 31.2 and $134.9 \pm 16.2\%$, respectively. For the IN-FR scheme, Figure 11 shows the wear index and mass loss in 250 cumulative cycles until reaching 1000 cycles. This coating had a lower wear index with a value of $272.7 \pm 6.4\%$. Thus, when comparing IN-FR to the C-FR coating, similar abrasion resistance properties were obtained. Although the C-FR coatings showed a lower index of abrasion wear with a value of $29.5 \pm 0.8\%$, the developed scheme showed mass losses of around $54.7 \pm 25.7\%$ after 1000 cumulative cycles. This indicates that the dual IN-FR protection system ensures that, after 1000 abrasion cycles, the substrate still retains its protection with at least one of the coating layers. Therefore, the IN-FR formulated paint scheme provides fire resistance and abrasion resistance properties.

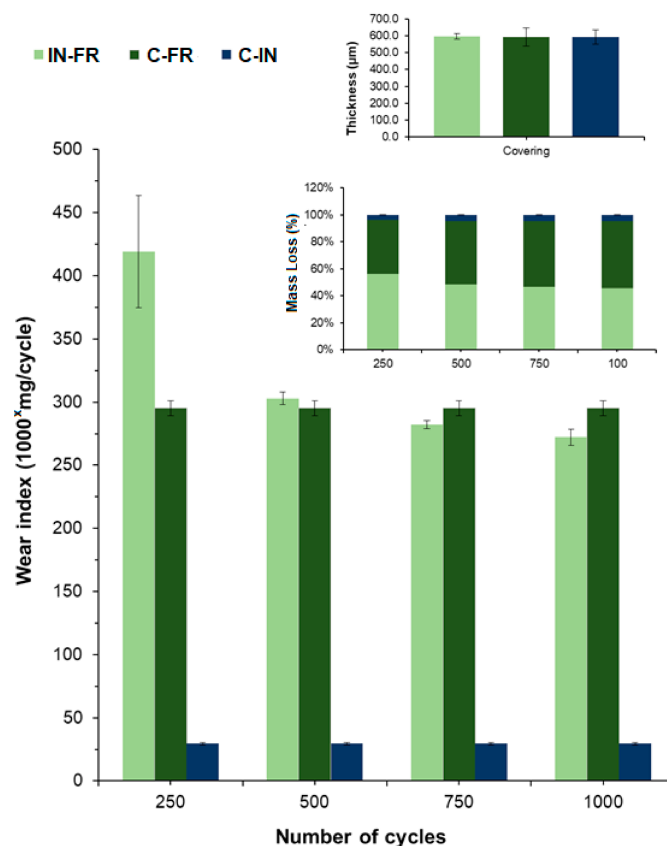


Figure 11. Wear index obtained by abrasion test for the dual scheme (IN-FR) on steel substrates compared to commercial coatings.

4. Conclusions

In this study, an active–passive two-layer coating scheme with both intumescent and fire-retardant properties was developed. In addition, tannins obtained from the waste of the *Pinus radiata* bark were demonstrated to be useful additives in the formulation of these fire-resistant coatings. The results show that H-MWTs can act as a carbon source, and their level of concentration in formulations was shown to be critical in achieving an intumescent or fire-retardant effect. When added in high proportions in the formulations, the tannins allowed for the formation of a carbonaceous foam layer by reacting with an acid catalyst. When low proportions were added, the formation of a fire-retardant carbon layer occurred. The combination of an IN layer and an FR (FR: Flame retardant coating) layer in a coating scheme showed better fire-resistance results compared to the commercial products, as well as better results than the IN or FR layer individually. The IN-FR scheme presented good mechanical properties at the same application thicknesses as those of commercial ones and can be used in both wood and steel.

Supplementary Materials: The following are available online at <https://www.mdpi.com/article/10.3390/coatings11040460/s1>, Table S1. Variation of percentage compositions of PER, ME, and MAP on basic formulation, Figure S1: Fire response and foaming of (A) uncoated wood, (B) coating with SPP as catalyst (BF-SPP), and (C) MAP as catalyst (BF-MAP), Figure S2: Intumescence properties according to the variation of the basic components of the formulation, Figure S3: Water absorbed by H-MWT and L-MWT in periods between 8 and 264 h, Figure S4: Mass loss and carbonization index of (A) intumescent (FT5) and (B) fire-retardant (FT1) coatings, Figure S5: Resistance to detachment by adherence of the dual scheme on metal substrates with respect to the respective commercial coating, Figure S6: Abrasion test for fire-retardant (FR) and intumescent (IN) coatings on metal with increasing thickness.

Author Contributions: Methodology, A.D.-G., M.E.B. and J.R.; formal analysis, M.E.B., K.F. and M.F.M.; investigation, F.S.-P., M.F.M., D.R. and E.P.-T.; resources, K.F., M.F.M., F.S.-P. and E.P.-T.; writing—original draft preparation, A.F.J., M.E.B. and M.F.M.; writing—review and editing, A.F.J., M.E.B. and M.F.M.; project administration, M.F.M. and A.D.-G. All authors have read and agreed to the published version of the manuscript.

Funding: This work was funded by ANID FONDEQUIP Project N°EQM150139, PIA/APOYO CCTE AFB170007, and project FONDEF IDEA ID17110333.

Institutional Review Board Statement: Not applicable.

Informed Consent Statement: Not applicable.

Data Availability Statement: The data is contained in the article and the Supplementary Material File.

Acknowledgments: The authors would like to thank the Interdisciplinary Group of Advanced Nanocomposites (Grupo Interdisciplinario de Nanocompuestos Avanzados, GINA) of the Department of Engineering Materials (DIMAT, according to its Spanish acronym), Engineering School of the University of Concepción, for its laboratory of nanospectroscopy (LAB-NANOSPECT). A.F.J. would like to thank the University of La Frontera. National Agency for Research and Development of Chile (ANID) by project: FONDEF Project N° ID17110333, PIA/APOYO CCTE AFB170007. MFM would like to thank Valentina Lamilla for her enormous support.

Conflicts of Interest: The authors declare no conflict of interest.

References

1. Yew, M.C.; Sulong, N.R. Fire-resistive performance of intumescent flame-retardant coatings for steel. *Mater. Des.* **2012**, *34*, 719–724. [[CrossRef](#)]
2. Jaramillo, A.; Díaz-Gómez, A.; Ramirez, J.; Berrio, M.; Cornejo, V.; Rojas, D.; Montoya, L.; Mera, A.; Melendrez, M. Eco-Friendly Fire-Resistant Coatings Containing Dihydrogen Ammonium Phosphate Microcapsules and Tannins. *Prog. Org. Coat.* **2021**, *11*, 280. [[CrossRef](#)]
3. Liang, S.; Neisius, N.M.; Gaan, S. Recent developments in flame retardant polymeric coatings. *Coatings* **2013**, *76*, 1642–1665. [[CrossRef](#)]
4. Baldissera, A.F.; Silveira, M.R.; Dornelles, A.C.; Ferreira, C.A. Assessment of lignin as a carbon source in intumescent coatings containing polyaniline. *J. Coat. Technol. Res.* **2020**, *17*, 1–11. [[CrossRef](#)]
5. Lu, H.; Song, L.; Hu, Y. A review on flame retardant technology in China. Part II: Flame retardant polymeric nanocomposites and coatings. *Polym. Adv. Technol.* **2011**, *22*, 379–394. [[CrossRef](#)]
6. Yew, M.; Sulong, N.R.; Amalina, M.; Johan, M. Influences of flame-retardant fillers on fire protection and mechanical properties of intumescent coatings. *Prog. Org. Coat.* **2015**, *78*, 59–66. [[CrossRef](#)]
7. Wang, Z.; Han, E.; Ke, W. Effect of nanoparticles on the improvement in fire-resistant and anti-ageing properties of flame-retardant coating. *Surf. Coat. Technol.* **2006**, *200*, 5706–5716. [[CrossRef](#)]
8. Weil, E.D. Fire-Protective and Flame-Retardant Coatings - A State-of-the-Art Review. *J. Fire Sci.* **2011**, *29*, 259–296. [[CrossRef](#)]
9. Oliveira, R.B.R.; Junior, A.L.M.; Vieira, L.C.M. Intumescent paint as fire protection coating. *Rev. IBRACON Estrut. Mater.* **2017**, *10*, 220–231. [[CrossRef](#)]
10. Shih, Y.; Cheung, F.; Koo, J. Theoretical Modeling of Intumescent Fire-Retardant Materials. *J. Fire Sci.* **1998**, *16*, 46–71. [[CrossRef](#)]
11. Amaral-Labat, G.; Szczurek, A.; Fierro, V.; Stein, N.; Boulanger, C.; Pizzi, A.; Celzard, A. Pore structure and electrochemical performances of tannin-based carbon cryogels. *Biomass-Bioenergy* **2012**, *39*, 274–282. [[CrossRef](#)]
12. Chou, C.-S.; Lin, S.-H.; Wang, C.-I. Preparation and characterization of the intumescent fire retardant coating with a new flame retardant. *Adv. Powder Technol.* **2009**, *20*, 169–176. [[CrossRef](#)]
13. Chen, X.; Hu, Y.; Jiao, C.; Song, L. Preparation and thermal properties of a novel flame-retardant coating. *Polym. Degrad. Stab.* **2007**, *92*, 1141–1150. [[CrossRef](#)]

14. Montoya, L.; Contreras, D.; Jaramillo, A.; Carrasco, C.; Fernández, K.; Schwederski, B.; Rojas, D.; Melendrez, M. Study of anticorrosive coatings based on high and low molecular weight polyphenols extracted from the Pine radiata bark. *Prog. Org. Coat.* **2019**, *127*, 100–109. [[CrossRef](#)]
15. Jaramillo, A.; Montoya, L.; Prabhakar, J.M.; Sanhueza, J.; Fernández, K.; Rohwerder, M.; Rojas, D.; Montalba, C.; Melendrez, M. Formulation of a multifunctional coating based on polyphenols extracted from the Pine radiata bark and functionalized zinc oxide nanoparticles: Evaluation of hydrophobic and anticorrosive properties. *Prog. Org. Coat.* **2019**, *135*, 191–204. [[CrossRef](#)]
16. Da Silveira, M.R.; Peres, R.S.; Moritz, V.F.; Ferreira, C.A. Intumescent Coatings Based on Tannins for Fire Protection. *Mater. Res.* **2019**, *22*, 22. [[CrossRef](#)]
17. Chen, X.; Jiao, C. Thermal degradation characteristics of a novel flame retardant coating using TG-IR technique. *Polym. Degrad. Stab.* **2008**, *93*, 2222–2225. [[CrossRef](#)]
18. Ji, W.; Hua, S.W.; Miao, Z.; Zhen, C. Study and Prediction for the Fire Resistance of Acid Corroded Intumescent Coating. *Procedia Eng.* **2014**, *84*, 524–534. [[CrossRef](#)]
19. Bocalandro, C.; Sanhueza, V.; Gómez-Caravaca, A.M.; González-Álvarez, J.; Fernández, K.; Roedel, M.; Rodríguez-Estrada, M.T. Comparison of the composition of Pinus radiata bark extracts obtained at bench- and pilot-scales. *Ind. Crop. Prod.* **2012**, *38*, 21–26. [[CrossRef](#)]
20. Ma, W.; Waffo-Téguo, P.; Pissoni, M.A.; Jourdes, M.; Teissedre, P.-L. New insight into the unresolved HPLC broad peak of Cabernet Sauvignon grape seed polymeric tannins by combining CPC and Q-ToF approaches. *Food Chem.* **2018**, *249*, 168–175. [[CrossRef](#)]
21. Yang, T.; Dong, M.; Cui, J.; Gan, L.; Han, S. Exploring the formaldehyde reactivity of tannins with different molecular weight distributions: Bayberry tannins and larch tannins. *Holzforschung* **2020**, *74*, 673–682. [[CrossRef](#)]
22. Banach, M.; Makara, A. Thermal Decomposition of Sodium Phosphates. *J. Chem. Eng. Data* **2011**, *56*, 3095–3099. [[CrossRef](#)]
23. Jiang, H.-C.; Lin, W.-C.; Hua, M.; Pan, X.-H.; Shu, C.-M.; Jiang, J.-C. Analysis of kinetics of thermal decomposition of melamine blended with phosphorous ionic liquid by green approach. *J. Therm. Anal. Calorim.* **2017**, *131*, 2821–2831. [[CrossRef](#)]
24. Su, C.-H.; Chen, C.-C.; Liaw, H.-J.; Wang, S.-C. The Assessment of Fire Suppression Capability for the Ammonium Dihydrogen Phosphate Dry Powder of Commercial Fire Extinguishers. *Procedia Eng.* **2014**, *84*, 485–490. [[CrossRef](#)]
25. Pardo, A.; Romero, J.; Ortiz, E. High-temperature behaviour of ammonium dihydrogen phosphate. *J. Phys. Conf. Ser.* **2017**, *935*, 935. [[CrossRef](#)]
26. Venkitaraj, K.; Suresh, S. Experimental thermal degradation analysis of pentaerythritol with alumina nano additives for thermal energy storage application. *J. Energy Storage* **2019**, *22*, 8–16. [[CrossRef](#)]
27. Venkitaraj, K.; Suresh, S. Experimental study on thermal and chemical stability of pentaerythritol blended with low melting alloy as possible PCM for latent heat storage. *Exp. Therm. Fluid Sci.* **2017**, *88*, 73–87. [[CrossRef](#)]
28. Lim, W.P.; Mariatti, M.; Chow, W.; Mar, K. Effect of intumescent ammonium polyphosphate (APP) and melamine cyanurate (MC) on the properties of epoxy/glass fiber composites. *Compos. Part B Eng.* **2012**, *43*, 124–128. [[CrossRef](#)]
29. Xia, Y.; Jin, F.; Mao, Z.; Guan, Y.; Zheng, A. Effects of ammonium polyphosphate to pentaerythritol ratio on composition and properties of carbonaceous foam deriving from intumescent flame-retardant polypropylene. *Polym. Degrad. Stab.* **2014**, *107*, 64–73. [[CrossRef](#)]
30. Braghiroli, F.; Fierro, V.; Pizzi, A.; Rode, K.; Radke, W.; Delmotte, L.; Parmentier, J.; Celzard, A. Reaction of condensed tannins with ammonia. *Ind. Crop. Prod.* **2013**, *44*, 330–335. [[CrossRef](#)]
31. Yang, T.-T.; Guan, J.-P.; Tang, R.-C.; Chen, G. Condensed tannin from Dioscorea cirrhosa tuber as an eco-friendly and durable flame retardant for silk textile. *Ind. Crop. Prod.* **2018**, *115*, 16–25. [[CrossRef](#)]
32. Tudor, E.M.; Barbu, M.C.; Petutschnigg, A.; Réh, R. Added-value for wood bark as a coating layer for flooring tiles. *J. Clean. Prod.* **2018**, *170*, 1354–1360. [[CrossRef](#)]
33. Puri, R.G.; Khanna, A. Effect of cenospheres on the char formation and fire protective performance of water-based intumescent coatings on structural steel. *Prog. Org. Coat.* **2016**, *92*, 8–15. [[CrossRef](#)]
34. Yin, J.J.K.; Yew, M.C.; Saw, L.H.; Yew, M.K. Preparation of Intumescent Fire Protective Coating for Fire Rated Timber Door. *Coatings* **2019**, *9*, 738. [[CrossRef](#)]